



HAL
open science

Microscale thermophoresis for studying protein-small molecule affinity: Application to hyaluronidase

Rouba Nasreddine, Reine Nehmé

► **To cite this version:**

Rouba Nasreddine, Reine Nehmé. Microscale thermophoresis for studying protein-small molecule affinity: Application to hyaluronidase. *Microchemical Journal*, 2021, 170, pp.106763. 10.1016/j.microc.2021.106763 . hal-04758194

HAL Id: hal-04758194

<https://hal.science/hal-04758194v1>

Submitted on 13 Nov 2024

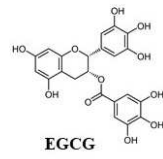
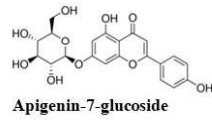
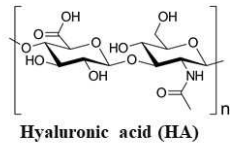
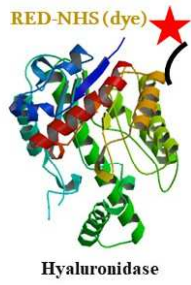
HAL is a multi-disciplinary open access archive for the deposit and dissemination of scientific research documents, whether they are published or not. The documents may come from teaching and research institutions in France or abroad, or from public or private research centers.

L'archive ouverte pluridisciplinaire **HAL**, est destinée au dépôt et à la diffusion de documents scientifiques de niveau recherche, publiés ou non, émanant des établissements d'enseignement et de recherche français ou étrangers, des laboratoires publics ou privés.

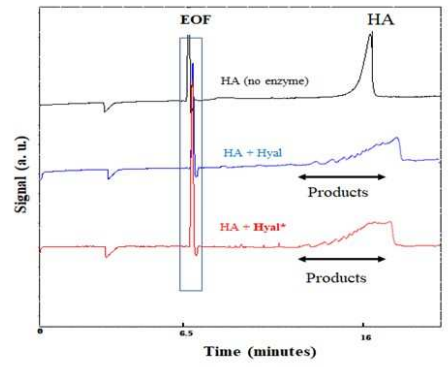


Distributed under a Creative Commons Attribution - NonCommercial 4.0 International License

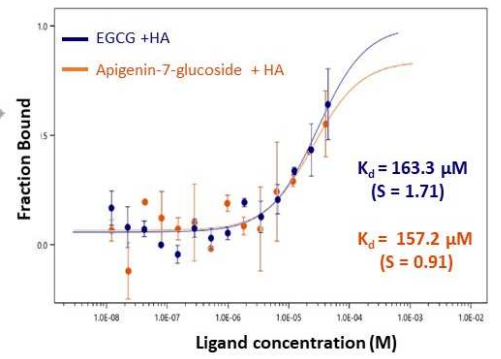
41 Graphical abstract



Post labelling activity check by Capillary Electrophoresis (CE)



Binding affinity by MicroScale Thermophoresis (MST)



42

43

44 **1 Introduction**

45 Enzyme interactions with small molecules such as solvent, substrate, co-factor or inhibitor has drawn an
46 increasing attention in developing new drugs, elucidating complex biological pathways or in therapy-associated
47 diagnosis. The difference of the size and the molecular weight between the studied partners make the
48 biomolecular interactions very challenging to determine and require sensitive techniques to detect the slightest
49 variation that occur upon binding. Several techniques defined as non-separative have been previously described
50 for the determination of the affinity constant of enzyme – small molecule systems such as isothermal titration
51 calorimetry (ITC) [1–4], surface plasmon resonance (SPR) [5–8], nuclear magnetic resonance (NMR) [9–12],
52 analytical ultracentrifugation (AUC) [13,14], fluorescence polarization (FP) and fluorescence anisotropy (FA)
53 [15–17]. These methods vary in terms of high-throughput ability, complexity, and the amount of needed sample.
54 Despite their robustness and reproducibility, ITC, AUC, and NMR can have mainly significant time and sample
55 demands which is less adequate for enzymatic studies due to the scarcity of these samples. SPR requires the
56 immobilization of enzyme, substantial experimental design efforts and proper treatment of surface during data
57 analysis. For FP and FA experiments, they are limited by the lifetimes of the fluorophores and can suffer from
58 autofluorescence and light scattering issues. The two separative techniques, high-performance affinity
59 chromatography (HPAC) [18–20] and capillary electrophoresis (CE) [21–27], have been also reported in the
60 literature to determine the biomolecular interactions of enzymes with small molecules. Despite its efficiency to
61 determine the binding affinity between investigated partners and the possibility of carrying out studies with
62 complex samples (crude plant extract for example), HPAC requires the preparation of the stationary phase, and
63 the immobilization of enzyme can affect its interaction with studied ligands in an uncontrolled manner. CE is a
64 well-established and versatile technique having several advantages including high resolving efficiency, short
65 analysis times and very small amounts of injected sample which is very suitable for enzymatic studies.
66 Nevertheless, to determine the binding affinity of investigated partners, five CE modes have been reported
67 namely zone migration (CZE), affinity CE (ACE), frontal analysis (FA), Hummel-Dreyer method (HD) and
68 vacancy peak (VP) [21]. The appropriate mode is selected based on the strength of the existing biomolecular
69 binding, the significant difference in electrophoretic mobility of the different components and the suitability of
70 buffer compositions towards the capillary inner coating. In addition to the complexity to establish experimental
71 conditions, CE suffers from fluctuations of electrophoretic mobilities making it less commonly used for affinity
72 studies [21].

73 Microscale thermophoresis or MST is one of the newest biophysical methods commercially available to
74 characterize biomolecular affinities. MST has several advantages over other non-separative analytical technique.
75 It is simple, requires low sample volume consumption, rapid (K_d obtained in less than 30 min), very sensitive
76 (pM) and immobilization-free. Moreover, MST offers the possibility to assess biomolecular interactions between
77 a large variety of partners of various molecular sizes with free choice of buffer composition in addition to
78 carrying out studies in biological liquids [28–33]. Biomolecular interactions of protein-protein, protein-nucleic
79 acids, protein-sugars, nucleic acid-nucleic acid and protein-small molecule have been reported using MST as
80 analytical tool as reviewed by Asmari *et al.*[34]. MST experiments are carried out in transparent thin capillaries
81 in which spatial migration of labelled molecules is monitored in a small volume of the capillary using confocal
82 microscope (Fig.S1a). This monitoring requires that one of the molecules under study be fluorescent in the visual
83 spectrum by using the molecule's intrinsic fluorescence when available or by adding extrinsic fluorophore [35].

84 The thermophoretic movement of molecules along the temperature gradient is initiated by illuminating the thin
85 glass capillary with infrared (IR) laser at $\lambda=1480$ nm which increases the inner temperature 2 to 6°C. The change
86 in fluorescence signal is recorded as a function of time (few seconds) and then the IR laser is extinguished
87 (Fig.S1a). A comparison of the tracked fluorescence before and sometime after the actuation of the IR laser,
88 defined respectively by cold region (blue zone) and hot region (red zone), is quantified as thermophoresis as
89 showed in Fig.S1b. The MST provides access to information relating to stoichiometry, the thermodynamic
90 dissociation constant, the enthalpy of one or more interacting partners and to visualize possible changes in
91 partner conformation. Following the MST trace of different scanned solutions allows one to determine if the
92 target was bounded or not (Fig.S1b) whereas the fluorescence signal shape reveals information on the protein's
93 solubility in the prepared solutions (Fig.S1c) [35].

94 Using MST, a binding affinity study was conducted for the first-time between a model commercially available
95 enzyme (EC.3.2.1.35), the hyaluronidase, and two of its inhibitors, the epigallocatechin gallate (EGCG) and the
96 apigenin-7-glucoside. The inhibitory effect of these two natural compounds towards hyaluronidase was
97 previously confirmed by CE. Hyaluronidase is a family of very dissimilar enzymes that degrade hyaluronic acid
98 (HA), a non-sulphated glycosaminoglycan very abundant in extracellular matrix of all tissues and body fluids
99 [36–38]. The size and the abundance of HA are very important for its function and studies have shown that low
100 molecular weight is involved in large number of physiological and pathological processes. Preventing HA's
101 fragmentation by reducing the enzyme activity using natural products as inhibitors is becoming a very attractive
102 way to ensure its protective function for treatment purposes such as cancer, lung injury and osteoarthritis [39–41]
103 or for cosmetic applications such as wound healing or dermal fillers [42–44]. The hyaluronidase kinetics were
104 previously studied in our laboratory using pre-capillary CE assay [45–47]. The HA hydrolysis by hyaluronidase
105 after 180 min of incubation time resulted in low molecular oligomers where the final product of the HA
106 hydrolysis reaction is tetrasaccharide. The peak identification of different products was carried out by CE/HRMS
107 requiring hence the use of volatile buffer either for incubation buffer (sodium acetate pH 4) or as background
108 electrolyte (BGE) (ammonium acetate pH 9). The kinetic degradation rate of HA over time was very slow with a
109 maximum reached after 100 min. The overall reaction mechanism is a complex process since the HA
110 degradation mechanism is constituted of successive cleavage and recombination steps of intermediate oligomers
111 which are also hyaluronidase's substrate. To better understand the working mechanism, we have recently
112 developed a full comprehensive kinetic model for the late stage of HA hydrolysis which demonstrated the
113 complexity of the enzymatic reaction by the formation of active and inactive dimers [48]. On the other hand,
114 using CE enzymatic based assay, the hyaluronidase activity in the presence of numerous molecules or plant
115 extracts was evaluated by following the tetrasaccharide peak's area. Results have showed that the hyaluronidase
116 activity was reduced by 20% in the presence of polyethylene glycol. Small natural molecules such as EGCG,
117 quercotriterpenoside-I and apigenin-7-glucoside in addition to original synthetic chondroitin sulfate
118 tetrasaccharides also reduced the hyaluronidase activity between 37 % for this latter and 98% for EGCG, the
119 referenced hyaluronidase inhibitor. Nevertheless, the inhibition mechanism of hyaluronidase by EGCG and
120 apigenin-7-glucoside, the selected small flavonoid molecules [46,47] is not well described in the literature.
121 Therefore, a systematic study was conducted, and the main experimental parameters investigated were the nature
122 of the buffer and its composition to carry out labelling and MST analysis. CE/UV was used as a complementary

123 technique to check the enzyme's activity after labelling. Once all parameters were defined, a full titration of each
124 inhibitor was carried out and the dissociation constant K_d was determined.

125

126 **2 Materials and methods**

127 **2.1 Chemicals**

128 All reagents were of analytical grade and used as received without further purification. Ammonium acetate
129 ($\text{CH}_3\text{COONH}_4$, purity $\geq 98\%$), epigallocatechin gallate (EGCG, purity $\geq 95\%$), apegenin-7-glucoside
130 ($\text{C}_{21}\text{H}_{20}\text{O}_{10}$, purity $\geq 97\%$), hyaluronidase type I-S from bovine testes (Hyal, 400-1000 units.mg⁻¹ solid), sodium
131 acetate (CH_3COONa , purity $\geq 99\%$), Tween-20 (10% v/v), sodium hydroxide (NaOH, purity $\geq 98\%$), sodium
132 chloride (NaCl, analytical grade, purity $\geq 99.5\%$) and bovine serum albumin (BSA, purity $\geq 98\%$) were
133 purchased from Sigma-Aldrich (Saint-Quentin Fallavier, France). Sodium dihydrogen phosphate dihydrate (Na
134 $\text{H}_2\text{PO}_4 \cdot 2\text{H}_2\text{O}$, purity $\geq 97\%$) purchased from Prolabo, France. Hyaluronic acid, sodium salt, *Streptococcus*
135 *pyrogenes* (HA, CAS 9067-32-7 – Calbiochem) was purchased from Merck Millipore (Molsheim, France).
136 Dimethyl sulfoxide (DMSO), was purchased from Fisher scientific ($(\text{CH}_3)_2\text{SO}$, purity $\geq 99\%$). Ethanol absolute
137 (EtOH, $\text{H}_3\text{CCH}_2\text{OH}$, purity $\geq 99,7\%$), glacial acetic acid (CH_3COOH), ammonia (NH_4OH , purity = 28%), were
138 purchased from VWR International (Fontenay-sous-Bois, France). Deionized H_2O (18 M Ω -cm) produced by a
139 Purelab flex apparatus from Veolia (Aubervilliers, France). Syringes and hydrophilic polyvinylidenedifluoride
140 (PVDF) Millex-HV Syringe Filters, pore size 0.2 μm , were purchased from Merck Millipore. Monolith Protein
141 Labeling Kit RED-NHS 2nd Generation (Amine Reactive) purchased from NanoTemper Technologies GmbH-
142 Munich Germany.

143 **2.2 Buffer solutions**

144 All buffer solutions were freshly prepared every working day in deionized H_2O . Then, their pH was adjusted
145 before being filtered and stored at 4°C.

146 For capillary electrophoresis analyses, the background electrolyte (BGE) was prepared by dissolving the
147 appropriate amount of ammonium acetate in deionized H_2O to make 50 mM solution. The pH was adjusted to
148 8.9 with 1 M ammonia.

149 For MST experiments, different buffers presented in Table 1 were tested and are listed as follow:

150 **sodium acetate buffer** was prepared by dissolving the appropriate amount of sodium acetate salt in deionized
151 water to make a 2 mM solution and the pH was adjusted to 9.8 with 1 M ammonia for labelling step (buffer A)
152 and at pH 4 with 1 M glacial acetic acid (buffer B) for elution step to collect the labeled enzyme and to carry out
153 CE enzymatic assay. To this buffer, different additives (Tween -20, BSA or ethanol) were added at different
154 final concentrations to run MST experiments (buffer C).

155 **phosphate ammonium buffer** was prepared by dissolving the appropriate amount of sodium dihydrogen
156 phosphate dihydrate in deionized water to make 20 mM solution to which an appropriate amount of sodium
157 chloride was added to have 77 mM, then the pH was adjusted to 6.6 with 1 M ammonia (buffer D). This buffer
158 was used to carry out enzyme labelling, enzyme collection and CE assay. To this, Tween-20 was added at final
159 concentration of 0.05 % for MST experiments (buffer E).

160

161

162

163
164
165

Table 1 Buffers used to carry out hyaluronidase labelling as well as CE and MST experiments

Sodium acetate buffer		Phosphate ammonium buffer	
Buffer A (for Hyal labelling)	2 mM CH ₃ COONa (pH 9.8)	Buffer D (for CE and MST)	20 mM NaH ₂ PO ₄ ·2H ₂ O + 50 mM NH ₃ + 77 mM NaCl (pH 6.6)
Buffer B (for CE and MST)	2 mM CH ₃ COONa (pH 4.0)		
Buffer C (for MST)	Buffer B + additives* * (0.01% or 0.1% BSA; 0.05 % or 0.1% Tween -20; 5% or 10% ethanol)	Buffer E (for MST)	Buffer D + 0.05 % Tween-20

166

167 2.3 Stock solutions

168 HA stock solution was prepared in deionized H₂O at a concentration of 4.5 μM and then diluted to the
169 appropriate concentrations. Inhibitor stock solutions of EGCG and apigenin-7-glucoside were prepared at 15
170 mM in a mixed organic solvent of DMSO / ethanol 30 % / 70 % (v/v). To ensure total solubility, inhibitor
171 solutions were vortexed for 1 min and placed in an ultrasound bath for 5 min and then diluted to the desired
172 concentration in the selected buffer. Hyaluronidase stock solution used to carry out labelling was prepared at 10
173 μM in buffer A or buffer D (Table 1).

174

175 3 Instrumentation and operating conditions

176 3.1 Hyaluronidase labelling for MST and CE analyses

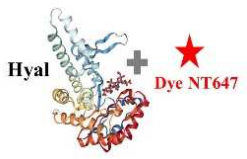
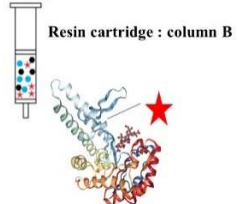
177 Before conducting MST experiments, hyaluronidase was labelled according to different steps summarized in
178 Table 2. Covalent fluorescence labelling of hyaluronidase was carried out following the protocol for N-
179 hydroxysuccinimide (NHS) coupling of the dye NT647 (Monolith NTTM Protein Labeling Kit RED-NHS 2nd
180 Generation, NanoTemper Technologies, Munich, Germany) to primary amine of lysine residue and its
181 preparation was performed according to the provider instructions. Briefly, the fluorophore NT647-NHS was
182 incubated at room temperature with the enzyme of initial concentration of 10 μM with a protein: dye ratio equal
183 to 1:3. The incubation time was reduced to 16 min instead of 30 min since the enzyme was over labelled (degree
184 of labelling, DOL, higher than 2.9) when it was incubated to 30 min. The enzyme was prepared in sodium
185 acetate buffer at pH 9.8 (buffer A) or in phosphate ammonium buffer at pH 6.6 (buffer D) (1st step in Table 2).
186 The labeling mixture was subsequently applied to the gravity flow columns B, a gel exclusion resin type, from
187 the Monolith NTTM Protein Labeling Kit RED-NHS 2nd Generation to remove the unbound fluorophores. Before
188 enzyme elution, column B was equilibrated with sodium acetate buffer at pH 4 (buffer B) or with phosphate
189 buffer at pH 6.6 (buffer D) (2nd step Table 2). After elution from the column, the concentration of the collected
190 labeled enzyme was quantified spectrophotometrically. A total volume of 550 μL of labeled enzyme was
191 recovered and aliquots of 50 μL were stored at -20 °C. The activity of the labeled enzyme was checked using CE
192 / UV before running MST experiments (3rd step in Table 2). For the rest of the study, labeled hyaluronidase is
193 defined as Hyal*.

194

195

196
197
198
199
200
201
202
203
204

Table 2 Experimental protocol to carry out binding affinity study. 1st step: labelling the hyaluronidase with RED NT647-NHS fluorophore provided by NanoTemper using buffer A or D followed by incubation in the dark at room temperature. 2nd step purification and collection of Hyal* using buffer B or D and then storage of collected enzyme as aliquots at -20°C. 3rd step: the analysis a) labelled enzyme, Hyal*, activity checked using CE at $\lambda=200$ nm and b) MST assay carried out by a serial dilution of inhibitor in buffer C or E; adding Hyal* at 5 nM and finally determining the dissociation constant K_d . Detailed buffer compositions are reported in Table 1.

	1 st step Hyaluronidase labelling	2 nd step Labelled Hyaluronidase (Hyal*) purification	3 rd step: Analyses	
			a) Monitoring of Hyal* catalysis activity by CE	b) MST binding assay Hyal*+inhibitor
Experimental protocol	 <p>→Incubation at room temperature for 15 min</p>	 <p>→Hyal*: storage at -20°C</p>	<p>Hyal* or Hyal + Substrate in the presence or absence of inhibitor</p> <p>→ In all cases: Following substrate and products peak intensity by CE/UV at 200 nm</p>	<p>(Hyal*+ inhibitor): serial dilution of 1:1 of inhibitor (16 capillaries) then Hyal* was added at fixed concentration of 5 nM.</p> <p>→Dissociation constant (K_d) determined at 37°C and 60% of excitation power</p>
Buffer used for labelling or to run CE / MST analysis (see Table1)	Buffer A or D	Buffer B or D	Buffer B or D	Buffer C or E

205

3.2 Hyaluronidase quantification using UV spectrophotometry

206
207 The concentration of the recovered labelled hyaluronidase from resin cartridge and DOL (2nd step in Table 2)
208 were determined using a double beam UV- visible spectrophotometer (UV1800, Shimadzu, Japan). Quartz cells
209 of 0.5 mL and 10 mm length were used to carry out the measurements. A full scan was carried out from 200 nm
210 to 750 nm. The obtained absorbance at 205 nm and 650 nm allowed the calculation of the concentration of the
211 collected labelled hyaluronidase using Eq.1 and then DOL was calculated according to Eq.2.

$$C(M) = \frac{A_{205} - (A_{650} \times C_f)}{31 \times MW} \quad \text{Eq. 1}$$

212 A_{205} : corrected absorbance of the peptide bonds at 205 nm; A_{650} : corrected maximum absorbance of the dye
213 NT647 at 650 nm.

214 C_f : is the correction factor of the dye NT647 to correct the absorbance of the peptide bonds at 205 nm (this
215 factor is equal to 0.19) and the extinction coefficient of the Hyal* at A_{205} (31).

216 MW : is the molecular weight of hyaluronidase ($g \text{ mol}^{-1}$).

217

218 The DOL indicates the amount of the dye bound to the enzyme, it was calculated according to Eq.2

$$DOL = \frac{A_{650}}{195\,000 (M^{-1}cm^{-1}) \times C(M)} \quad \text{Eq. 2}$$

219 195 000 is the molar absorbance of the dye NT647.

220 $C(M)$: concentration of the Hyal* calculated according to Eq.1.

221

222 **3.3 Capillary electrophoresis analysis to evaluate labelled hyaluronidase catalytic activity**

223 Hyal* activity was checked based on a protocol previously developed and optimized in our laboratory using pre-
224 capillary CE assays [45]. Briefly, 10 μL of HA (0.8 mg mL^{-1}) were mixed with 35 μL of incubation buffer
225 (buffer C or buffer D) and then 5 μL of enzyme solution (labeled or not) was added to the reaction mixture.
226 Enzymatic reactions were incubated at 37 $^{\circ}\text{C}$ for 180 minutes before being stopped by increasing the temperature
227 to 90 $^{\circ}\text{C}$ using a hot water bath for 10 minutes. The reaction mixtures were then analyzed on a PA 800+ (AB
228 Sciex, USA) CE apparatus equipped with a photodiode array detector. The final mixture was injected using
229 hydrodynamic injection at 1.5 psi for 5s from the anodic side. The separation of products from enzyme was
230 carried out by applying + 15 kV for 25 min and the detection was ensured at $\lambda = 200 \text{ nm}$. The CE control was
231 performed using the Beckman 32 karat software (Beckman Coulter, USA). Uncoated fused-silica capillaries
232 purchased from Polymicro Technologies (Phoenix, AZ, USA) were used with a total length of 57 cm (47 cm to
233 the detector) and 50 μm as inner diameter. Between the runs, the capillary was flushed with NaOH (5 min),
234 water (0.5 min) and BGE (3 min). All rinse cycles were carried out at 50 psi. Enzymatic reactions were repeated
235 twice for every tested condition and results were compared to those obtained with the unlabeled Hyal at the same
236 final concentration in the reaction mixture.

237 **3.4 MST binding analysis**

238 MST experiments were performed on the Monolith NT.115 Pico equipped with red filter purchased from
239 NanoTemper Technologies (GmbH, Munich, Germany) which ensure an excitation light at 605 – 645 nm and
240 signal was recorded at 680 – 685 nm emission wavelengths (Fig.1).

241 The apparatus design allows the analysis of up to 16 solutions leading to the determination of detailed K_d in a
242 single run in less than 30 min. To explore MST data easily, two output signals issued from MST software were
243 carefully followed, the fluorescence signal of each loaded and scanned solution and the corresponding MST
244 trace.

245

246 The dissociation constants (K_d) were determined using the K_d binding model based on the equation 3 (built-in
247 analysis in the MO.Binding affinity software from NanoTemper Technologies GmbH, München, Germany). The
248 equation 3 is based on the Langmuir binding isotherm and a 1:1 interaction model. The optimal time region to
249 assess binding was determined manually by selecting a region on the MST signal (Fig.S1 b) with a signal-to-
250 noise ratio superior to 5. The equation 3 is described as follows (for more details refer to [49,50]):

$$f_{(C)} = F_{norm(target)} + \frac{(F_{norm(complex)} - F_{norm(target)}) \times C + C_{target} + K_d - \sqrt{(C + C_{target} + k_d)^2 - 4 \times C \times C_{target}}}{2C_{target}} \quad \text{Eq.3}$$

251 Where $f(C)$ is the fraction bound at a given ligand concentration “C”. F_{norm} is the normalized fluorescence signal
252 which is defined by the ratio of relative fluorescence of the selected hot region and relative fluorescence of cold
253 region. $F_{norm(target)}$ is the normalized fluorescence signal of unbound Hyal* and $F_{norm(complex)}$ is the normalized
254 fluorescence signal of bounded Hyal* to the inhibitor. C_{target} is the final concentration of the target Hyal* in the
255 assay.

256 A systematic study was carried out before conducting the binding affinity analysis between Hyal* and the
257 inhibitors. Four parameters were verified: the fluorescence signal of Hyal* after being labelled with buffer A or
258 buffer D, the type of Monolith NTTM capillaries whether standard or premium coated capillaries, the enzyme

259 concentration and finally the absence of inhibitor and HA autofluorescence. Then, the dissociation constant, K_d ,
260 was determined in the presence and in the absence of the substrate. Experiments were designed to have the same
261 final concentrations of inhibitor and the enzyme in the final mixture in both cases.

262 *Hyal* fluorescence signal and buffer composition:* The fluorescence signal of Hyal* was checked after the
263 elution step to verify the labelling efficiency and to fix the IR illumination power for thermophoretic movement.
264 Consequently, Hyal* was diluted to the desired concentration in the selected buffer (C, D, or E see Table 1) and
265 loaded into Monolith NT™ capillaries of 4 μL capacity volume of standard or premium coated capillaries with a
266 preference for the former for a budgetary reason. Using sodium acetate buffer, different additives were tested to
267 improve fluorescence signal and MST trace; surfactant: Tween-20 at 0.05 % or 0.1%, organic solvent: EtOH at
268 5% or 10%, inert protein: BSA at 0.01 or 0.1% or mixed conditions of organic solvent and surfactant (buffer C
269 Table 1). For phosphate ammonium buffer, Tween-20 at 0.05% was only tested (buffer E).

270 *Hyal* concentration:* The fluorescence signal of four Hyal* concentrations 1, 5, 10 and 15 nM were compared to
271 select the appropriate Hyal* concentration to conduct the binding affinity assay. All concentrations were
272 prepared by diluting Hyal* stock solution in the selected buffer based on the initial concentration calculated
273 according to Eq.1.

274 *Hyal*- inhibitor binding assay:* The biomolecular interactions between Hyal* and selected inhibitors were
275 carried out in absence and in presence of HA, the substrate of hyaluronidase.

276 In the absence of HA, the experiments consisted of 16 - point titration series in which the inhibitor
277 concentrations were generated as a 1:1 dilution of the previous sample, to this 10 μL of the labelled enzyme,
278 Hyal*, was added to all vials at the same final concentration bringing the total volume of the mixture to 20 μL .

279 In the presence of HA, the total volume of the mixture was equal to 30 μL and composed of 10 μL of inhibitor
280 obtained by a serial dilution with the same method described above to which 10 μL of the substrate were added
281 at a constant concentration equal to $K_m = 0.4 \mu\text{M}$ [46] and finally 10 μL of Hyal* was added to have the same
282 final concentration (see 3rd step in Table 2). In both cases, the mixture was pre-incubated between 5 min and 120
283 min at 37°C allowing the formation of the complex, then mixtures were centrifuged at 10 000 x g for 10 min at
284 10°C to prevent overheating (BR4i multifunction centrifuge, thermo electron). Each binding assay was prepared
285 independently and repeated three times ($n = 3$). The standard deviation of the average of the three $f(C)$ values for
286 each concentration was calculated using the root mean squared error (RMSE) according to the following
287 Equation:

$$RMSE = \sqrt{\sum_i \frac{(m_i - y_i)^2}{v}} \quad \text{Eq.4}$$

288 With the residual degree of freedom $v=n-m$; n is the number of data points and m is the number of parameters
289 that are fitted (four parameters for both, K_d model, except any parameters are fixed). The y -values of the fitted
290 curves at position “ i ” are denoted by m_i and the actual data points are denoted by y_i .

291 The inhibitors concentration range was selected according to two parameters: the final percentage of organic
292 solvent in the mixture and the solubility of the inhibitor in the reaction media. In all cases and to ensure that the
293 same amount of Hyal* was added to all solutions, the raw fluorescence counts of 16 solutions was checked by
294 comparing their intensities which should range between +/- 20% of the average fluorescence value.

295

296

297

298 **4 Results and discussion**

299 To correctly conduct MST experiments, it is important to ensure that the hyaluronidase - inhibitor system can be
300 monitored and quantified accurately using suitable experimental conditions. For this, a systematic study of the
301 influence of different parameters was performed before conducting the bimolecular affinity of Hyal* and its
302 selected inhibitors and then evaluating the K_d values in the presence and in the absence of Hyal* substrate.

303 **4.1 Optimization of MST conditions**

304 Buffers used for labelling play a key role in all steps of MST experiments. They should be carefully chosen to
305 respect the efficiency of the dye binding during the labelling process and the stability of the enzyme by avoiding
306 its precipitation throughout the labelling procedure. In this context, three labelling attempts were carried out with
307 two different buffers (two attempts with buffer A and one attempt with buffer D) considering the effect of such
308 changing on hyaluronidase stability and activity. In fact, enzyme is more active and more stable at low pH and
309 ionic strength. When increasing the pH, additional salt must be added to maintain the same activity of
310 hyaluronidase as shown by Ablurn and Whitley [51].

311 The concentration of recovered Hyal* and DOL were calculated according to Eq.1 and 2. Then, MST test was
312 carried out to verify the MST traces and its fluorescence signal intensity. Finally, the buffer composition was
313 optimized to obtain the best fluorescence and MST signals by adding different additives as reported in Table 1.

314 **4.1.1 Sodium acetate buffer for hyaluronidase labelling and MST analysis**

315 The sodium acetate buffer was selected because it was used in our previous studies to establish hyaluronidase
316 enzymatic assay conditions for CE analysis [45,46]. To be consistent with the dye chemistry which requires an
317 alkaline pH ~8.2 to label efficiently the Hyal, the pH was set at 9.8 instead of 8.2 (buffer A in Table 1) to avoid
318 the enzyme precipitation. The pH was fixed at 9.8 since the isoelectric point of hyaluronidase is equal to 8.6.
319 Nevertheless, and in order to be able to compare results with those previously obtained with CE, the elution of
320 the labelled enzyme from the resin cartridge was performed with 2 mM sodium acetate buffer at pH 4 (buffer B
321 in Table 1) which is the same pH used in our previous CE work [45,46].

322 Using the buffer A, two labelling attempts of Hyal were carried out with two different incubation time, 15 min
323 and 30 min in the dark at room temperature (1st step in Table 2). Hyal* was then recovered as described in the
324 2nd step of Table 1. Finally, Hyal* concentration and its DOL were calculated according to Eq.1 and 2,
325 respectively.

326 Hyal* concentrations and DOL were calculated, using UV spectrophotometry, for the shorter incubation period
327 of 15 min as 632 nM and 0.3, respectively. For longer incubation period of 30 min, values were equal to 560 nM
328 and 2.9. As matter of fact, an ideal DOL value ranges between 0.5 and 1. A DOL value above 1 indicates that the
329 enzyme is over-labelled and may negatively affect the protein function. Furthermore, a value below 0.5 may
330 result in reduced signal-to-noise ratio (S/N) but can still be sufficient to carry out MST analyses given high
331 binding signals and an absence of photobleaching. Consequently, Hyal* obtained with 15 min incubation period
332 was chosen to carry out the rest of the study.

333 The labelling efficiency of Hyal* was verified by diluting the enzyme to 5 nM in buffer B, centrifuged at 10,000
334 x g for 10 min at 10°C, loaded into Monolith NTTM standard treated capillary and then analyzed at 25°C with an
335 auto detect of excitation power. The MST pre-test signal showed that intensity of signal was above 2500 counts

336 as preconized by the constructor, and the detected excitation power was equal to 60%. Nevertheless, using buffer
337 B as MST buffer provides distorted fluorescence signal (Fig.S2a-brown trace) and bumpy MST trace (Fig.S2b-
338 brown trace) indicating respectively the adsorption of the Hyal* onto the inner capillary wall and its aggregation
339 in the scanned solutions. To limit these disruptions, buffer B was supplemented by various additives at different
340 percentages as summarized in Table 1 having as a main goal a smooth MST trace and a symmetric gaussian
341 fluorescence signal. Moreover, the fixed goal was focused on using Monolith NT™ standard treated capillary
342 rather than the Monolith NT™ Premium coated one for budget issue since this latter is 3 times more expensive
343 than standard ones.

344 Firstly, using Monolith NT™ standard treated capillaries, the composition of buffer B was optimized using
345 Tween -20, a non-ionic surfactant aimed to increase enzyme solubility in the MST buffer and reduces its
346 adsorption on the inner capillary wall. Tween-20 was added at low percentage of 0.05% or 0.1%, nevertheless
347 aggregations were still detected. The same results were obtained when supplementing buffer B with EtOH at 5%
348 and 10% or with the presence of BSA at 0.01% or 0.1%. Furthermore, mixed conditions of 0.1% Tween- 20 +
349 0.01% BSA or 0.1% Tween-20 + 10% EtOH or 0.1%Tween-20 + 0.01% BSA + 5% EtOH did not eliminate
350 neither the Hyal* adsorption nor its aggregations (Fig.S2a and b). Finally, when using Monolith NT™ coated
351 capillaries with the same buffer additives to scan Hyal* at 5 nM, neither of output signals were improved as
352 shown in Fig.S2c and d.

353 To conclude, the sodium acetate buffer was not appropriate to carry out MST study since regardless the tested
354 conditions (buffer composition or capillary), the MST signals were always distorted. These observations may be
355 due to a change of pH during the labelling process reaching the isoelectric point of the hyaluronidase ($pI \approx 8.6$)
356 leading to its irreversible precipitation.

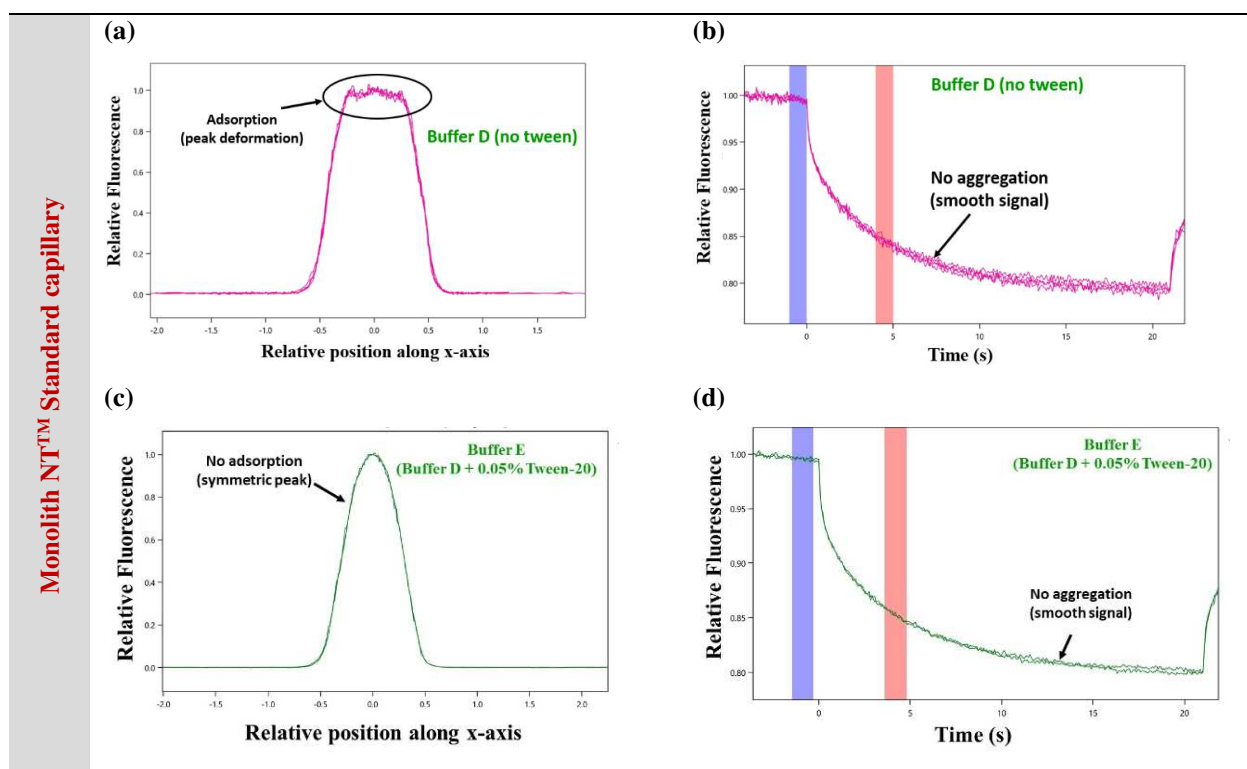
357 **4.1.2 Phosphate ammonium buffer for hyaluronidase labelling and MST analysis**

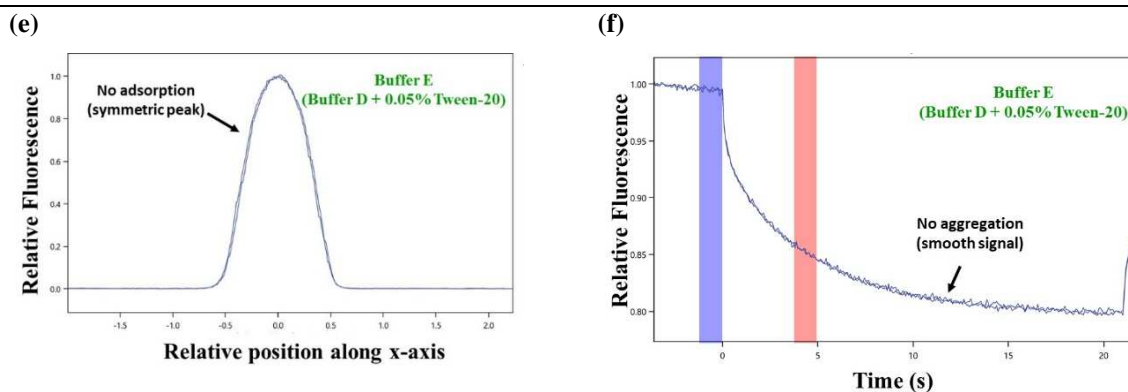
358 The third attempt to label the hyaluronidase was carried out using a phosphate ammonium-based buffer (20 mM
359 NaH_2PO_4 + 50 mM ammonia) + 77 mM NaCl at pH 6.6 aiming to improve the enzyme fluorescence signal shape
360 and its thermophoretic trace.

361 The same buffer was used to carry out hyaluronidase labelling (1st step in Table 2), purification and recovery (2nd
362 step in Table 2) and to also conduct biomolecular interactions after being optimized (3rd step in Table 2). The
363 incubation time of hyaluronidase with the dye was fixed at 15 min in the dark at room temperature to avoid
364 Hyal*'s over labelling. The recovered Hyal* concentration and the DOL were equal to 827 nM and 0.3,
365 respectively using Eq.1 and 2.

366 The obtained concentration of Hyal* with buffer D was 23% higher than Hyal* recovered with buffer B. The
367 differences in Hyal* concentration between both buffers arises from the fact that both buffers differ in their
368 respective compositions and pH. Both pH values are in the optimized range of hyaluronidase activity and
369 stability, nevertheless at higher pH, ionic strength must be increased to stabilize the enzyme as reported by
370 Alburn and Whitley [51]. Additionally, using buffer D to carry out hyaluronidase labelling and recovering
371 significantly prevented changing in pH during the process and hence increased the recovered Hyal* final
372 concentration. Nevertheless, the DOL was equal to the one calculated with the acetate buffer (around 0.3)
373 indicating that pH was not sufficient to have a DOL between 0.5 and 1. Despite this low DOL, MST
374 optimizations and experiments were carried out using this labelled Hyal*.

375 First, MST test was carried out to verify the efficiency of Hyal* by following the raw fluorescence counts of 5
 376 nM Hyal* diluted in buffer D and resulted in a raw fluorescence signal higher than 2500 counts with an
 377 excitation power of 60% indicating that Hyal* was sufficiently labeled using Monolith NT™ standard treated
 378 capillary. Nevertheless, the fluorescence signal shape indicates slight adsorption on the inner capillary wall
 379 (Fig.1a). The thermophoretic signals were smooth but slightly noisy as shown in Fig.1b. To improve these
 380 results using always the standard treated capillaries, the buffer composition was optimized by adding Tween-20
 381 at 0.05% (buffer E). Obtained results reported in Fig.1c and d showed that both signals (fluorescence and
 382 thermophoretic signals) of Hyal* prepared in buffer E were rectified indicating the absence of enzyme
 383 adsorption on the inner capillary wall and the total solubility of Hyal* inside the scanned solutions. Tween-20 at
 384 0.05% was ultimately chosen as additive to buffer D for future MST experiments as it demonstrated its potential,
 385 at a low concentration, to limit the Hyal* adsorption and making the MST trace smoother compared to results
 386 obtained with buffer D using standard treated capillaries. The same observations were obtained when 5 nM
 387 Hyal* solutions diluted in buffer E were scanned using Premium coated capillaries (Fig.1e and f).
 388 To conclude, phosphate ammonium-based buffer supplemented with 0.05% Tween-20 and standard treated
 389 capillaries are defined as optimum conditions which ensured total enzyme solubility with good MST signals
 390 permitting subsequently the conducting of Hyal*- inhibitors biomolecular interaction study.
 391





392 **Figure 1** Overlap of fluorescence signal of 5 nM Hyal* solutions (a, c, e) and the corresponding MST traces (b, d, f) loaded
 393 into Monolith NT™ standard treated capillaries (a, b, c and d) and Monolith NT™ Premium coated capillaries (e and f). 5
 394 nM of Hyal* prepared in buffer D (20 mM phosphate + 50 mM ammonia) + 77 mM NaCl at pH 6.6 without adding additives
 395 (a and b) and in buffer E (20 mM phosphate + 50 mM ammonia) + 77 mM NaCl at pH 6.6 + 0.05 % of Tween - 20 (c, d; e
 396 and f). Scans were recorded at 25°C and at 60 % of LED as excitation power.

397

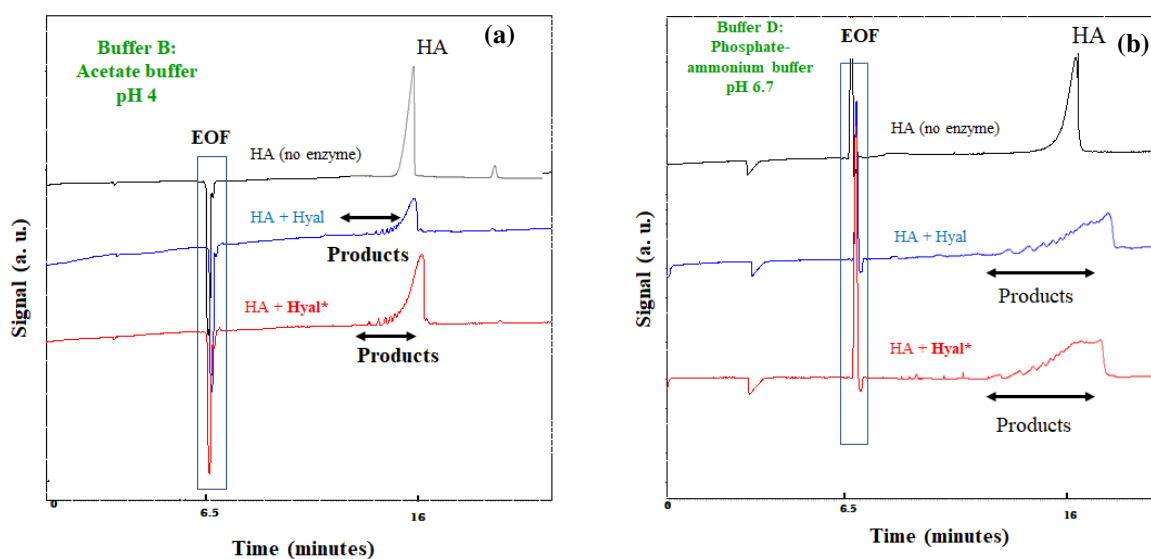
398 4.2 Labelled hyaluronidase catalytic activity assays by CE

399 As mentioned in the introduction section, hyaluronidase's working and inhibition mechanisms are complex
 400 processes. To ensure that labelling of the enzyme by adding an extrinsic fluorophore does not alter its function,
 401 the Hyal* activity was checked using pre-capillary CE assay according to the protocol described in section 3.3.
 402 More precisely, 5 μ L of the labelled enzyme was added to the mixture (total volume of 50 μ L) so that the final
 403 concentration of the enzyme was equal to 63.2 nM with acetate buffer (buffer B) and 82.7 nM with phosphate
 404 ammonium buffer (buffer D) according to the concentrations calculated with UV spectrophotometry (827 nM
 405 and 632 nM, respectively). Then, HA was added at a final concentration of 0.4 μ M and finally the mixture was
 406 incubated for 180 min before being stopped and analyzed by CE (more details in section 3.3). Labelled enzyme
 407 activity was compared with the respect to control assays run simultaneously where unlabeled enzyme prepared in
 408 the same selected buffer was added to the mixture at the same final concentration. Hyaluronic acid was also
 409 prepared in the same buffer used to collect the enzyme (2nd step in Table 2) at the same concentration of 0.4 μ M
 410 and it was injected using the same CE method.

411 Obtained results are reported in Fig.2. Electropherograms presented in Fig.2a and b, showed that gaussian HA
 412 peak shape obtained at 16 min when it was injected in the absence of enzyme is very different from the one in
 413 the presence of the enzyme. In fact, the electropherograms of enzymatic reactions carried out using both buffers
 414 (buffer B and buffer D) show that the reaction media contains mainly HA (peak at 16 min) with the formation of
 415 the HA hydrolysis oligomers. These products are presented as small peaks between 13 and 15 min, having
 416 molecular weights lower than the one of HA and they are negatively charged molecules since they appear after
 417 the electroosmotic flow (EOF=6.5 min) [38]. The peak at 13 min represents the tetrasaccharide, the final product
 418 of HA hydrolysis by hyaluronidase. Nonetheless, it is difficult to quantify it accurately.

419 These results confirm that the Hyal* remains active after being labelled regardless the labelling buffer even
 420 though the quantification of its activity is difficult. This observation is explained by the yield of the reaction
 421 which was very low since the amount of the enzyme presented in these tests (82 or 63 nM) were 40 to 50-fold
 422 lower, respectively, compared to the control CE-based assays [37]. These CE results demonstrate the
 423 preservation of the hyaluronidase activity despite the labelling step meaning that adding extrinsic dye did not
 424 affect the active site of the enzyme. On the other hand, CE choice as complementary technique to verify the

425 enzyme activity at low concentrations (tens of nM) has showed its efficiency and hence its superiority compared
 426 to other conventionnel techniques namely UV spectroscopy.
 427



428 **Figure 2** Electropherograms of HA hydrolysis showing the preservation of hyaluronidase activity after labelling using two
 429 different hyaluronidase labelling buffers. (a) Sodium acetate buffer at pH 4.0 (buffer B) and (b) phosphate-ammonia buffer at
 430 pH 6.6 (buffer D). Reaction mixture composition in buffer B and buffer D: 63.2 nM and 82.7 nM of hyaluronidase,
 431 respectively and HA was added at 0.4 μ M in both buffers. Offline CE assay conditions: incubation at 37°C for 180 minutes.
 432 IB: 2 mM sodium acetate (pH 4.0) or 20 mM sodium phosphate +50 mM ammonia + 77 mM NaCl (pH 6.6). CE analysis
 433 conditions: electrophoretic separation conditions: BGE: 50 mM ammonium acetate (pH 8.9); anodic injection: 1.5 psi for 5 s;
 434 separation: +15 kV at 25°C; detection: $\lambda = 200$ nm; rinse between analyses at 30 psi: 5 min NaOH (1 M), 0.5 min water and 3
 435 min BGE; bare-silica capillary: 57 cm total length, 47 cm detection length, 50 μ m i.d. EOF: electroosmotic flow.

436

437 4.3 Hyal* concentration for MST experiments and reagent autofluorescence

438 The appropriate concentration of Hyal* to be used for MST analyses was chosen by comparing the fluorescence
 439 signal intensities and the thermophoretic traces of four Hyal* concentration; 1, 5, 10 and 15 nM diluted in buffer
 440 D. The intensities of the fluorescence responses observed for 1 nM was less than 1000 counts in addition its
 441 noisy thermophoretic traces hindered the interpretation of the results and was thus inappropriate for future MST
 442 analyses (Fig.S3a and b). Hyal* concentration equal to 15 nM exhibited an important fluorescence signal (\approx
 443 6000 counts) and good MST trace. Nevertheless, the fluorescence signal peak presented a deformation in its
 444 shape indicating a slight adsorption on the inner wall of standard capillary (Fig.S3a). Conversely, the
 445 fluorescence intensity of both 5 nM and 10 nM of Hyal* were higher than 2500 counts which was largely
 446 sufficient for MST analyses and their corresponding thermophoretic traces were smooth as shown in Fig.S3a and
 447 b. Consequently, and for economic concerns, the concentration of 5 nM was chosen to carry out the binding
 448 affinity study with inhibitors. It is worth mentioning that this very low concentration of Hyal* is almost 600-fold
 449 lower than that used during the CE-UV enzymatic activity assays (3.33 μ M)
 450 Moreover, to confirm that the changing in thermophoretic signals when carrying binding affinity study is only
 451 due to Hyal* state *i.e.* bound or unbound, the autofluorescence of EGCG, apigenin-7-glucoside (prepared in
 452 buffer E at 1000 μ M) as well as the substrate HA (prepared in buffer E at 0.4 μ M) was verified. Results
 453 presented in Fig.S4 reveal a negligible raw fluorescence signal of EGCG, apigenin-7-glucoside and HA
 454 (around 500 counts).

455 **4.4 Biomolecular interactions of Hyal* - inhibitor system**

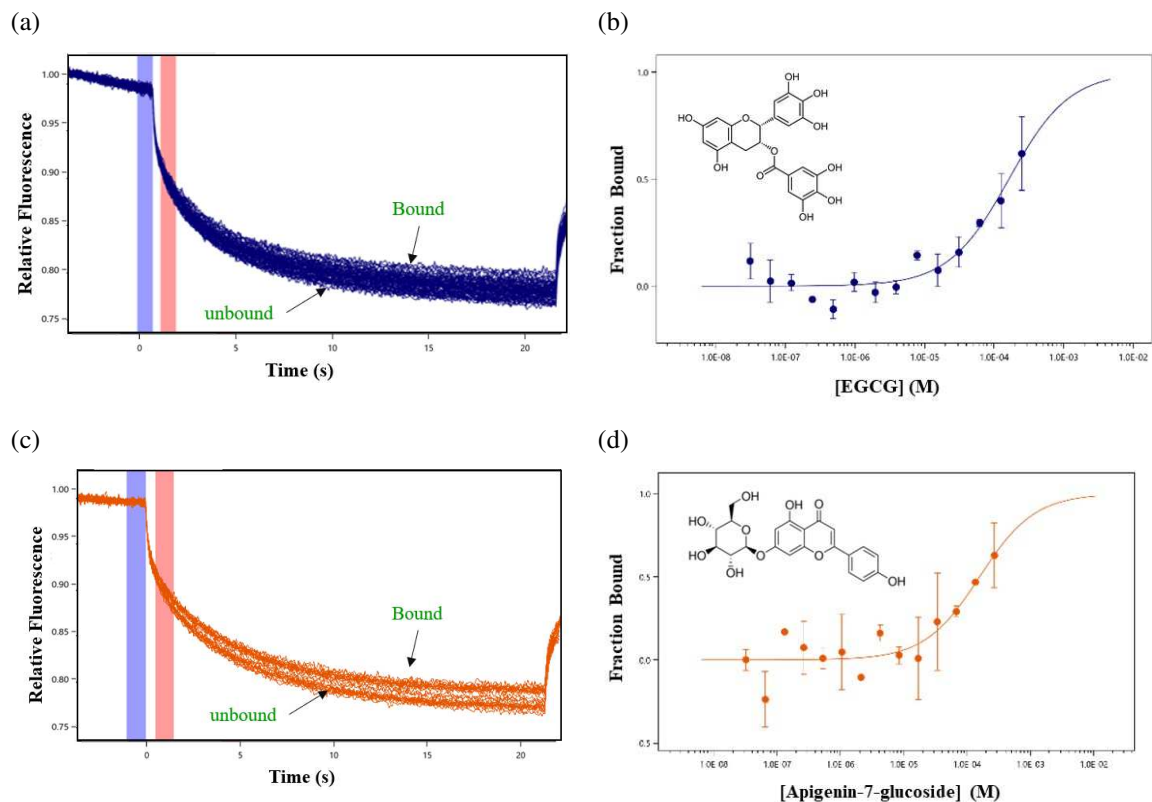
456 The optimized MST assay was applied to evaluate the biomolecular interaction of EGCG and apigenin-7-
457 glucoside towards Hyal*. The MST scans were carried out at 25°C and 37°C and thermophoretic response
458 curves were alike with no detection of adsorption or aggregation. To compare MST results with CE ones, the
459 MST analyses were recorded at 37°C and the Hyal*-ligand solutions were incubated for 5 min to 120 min also at
460 37°C which corresponds to the optimal temperature of Hyal's catalytic activity. Since the MST signal was not
461 influenced by the pre-incubation time, 5 min-time was selected for the following experiments.

462 First, when Hyal* was incubated with EGCG or with apigenin-7-glucoside, MST results did not reveal any
463 interaction between tested partners regardless of the concentration of inhibitors or the incubation times used.
464 This was completely unexpected since these molecules are known as potent inhibitors of hyaluronidase. In our
465 previous work using CE where the inhibitor was added to Hyal – HA system, the IC₅₀ which corresponds to a
466 reduction of 50% of Hyal activity was evaluated by following the peak area value of the tetrasaccharide (see
467 section 1). IC₅₀ of both molecules, were found to be equal to 0.02 mg mL⁻¹ (43.63 μM) and 0.07 mg mL⁻¹
468 (161.88 μM) for EGCG and apigenin-7-glucoside, respectively [47].

469 Consequently, the experimental conditions were then adjusted to be closer to those applied in CE analysis and
470 Hyal* was incubated either with EGCG or apigenin-7-glucoside in the presence of the substrate, HA at 0.4 μM.
471 The affinity study using the aforementioned conditions was possible since the kinetic degradation of HA by
472 hyaluronidase was slow (more details in section 1). During the 12 minutes needed to scan all of 16 capillaries
473 and the 5 min of pre-incubation, the HA's hydrolysis is negligible as shown in our previous study based on CE
474 [45,48]. In these conditions, the MST traces as well as the fraction bound curve to evaluate K_d for the binding
475 affinity analysis of the EGCG and apigenin-7- glucoside are presented in Fig.3. With both ligands, the
476 thermophoretic traces of all scanned solutions presented in Fig.3a and c showed a successive decline in signal
477 indicating that enzyme state was changing and varied from free enzyme (unbounded) to bounded one.
478 Additionally, the binding curve was a sigmoid with a well-defined lower plateau (Fig.3b and d). The MST traces
479 demonstrate differences between the high and low concentrations in response to thermophoresis. Despite that
480 Hyal*/ HA/ inhibitor complex saturation plateau was not completely formed for both inhibitors, K_d of EGCG
481 binding in presence of HA was evaluated from the binding curve as 163.3 μM with S/N = 17 and a standard error
482 of regression (S) equal to 1.71 (equations 3 and 4). For apigenin-7-glucoside with HA, K_d was equal to 157.2
483 μM with a S/N = 10 and a S = 0.91 (equations 3 and 4). Error bars on the figures represent standard deviation of
484 the average of three values of f(C) obtained for each concentration. It can be noticed that these errors are
485 relatively high for some experiments probably due to the purity of the labelled enzyme. Further experiments
486 need to be carried on for a better understanding of this variation.

487 The obtained results pointed out that the presence of HA, the enzyme substrate, in the final mixture was
488 mandatory to visualize the binding affinity between Hyal* and EGCG or Hyal* and apigenin-7-glucoside
489 suggesting that EGCG and apigenin-7-glucoside prompt a mixed inhibition mechanism of hyaluronidase [52].
490 The same observation was reported by Patil *et al.* [53] who have concluded that the inhibition mechanism of
491 hyaluronidase by quercetin, a small flavonoid molecule similar to those tested in our study, is more complex than
492 a classical competitive or uncompetitive inhibition since inhibitor affects both K_m and V_{max} values. Tomohara *et*
493 *al.* [54] also shared the same conclusion on epicatechin molecule by suggesting the presence of a specific type of
494 interaction with hyaluronidase causing negative allosteric effects on catalytic site.

495
496
497
498
499



500 **Figure 3** Thermophoretic traces (a and c) and dose-response curves (b and d) of Hyal*+ HA+ EGCG (a and b) and Hyal*+
501 HA+ apigenin-7-glucoside (c and d). Solutions prepared as follow: 16 solutions were obtained by performing a 1:1 serial
502 dilution of inhibitors in the concentration range of 1000 μM – 61 nM; the enzyme substrate HA was added to all preparations
503 at a constant concentration equal to 0.4 μM before adding Hyal* at 5 nM. Solutions were then incubated for 5 min,
504 centrifuged at 10 000 \times g at 10°C before being loaded into Monolith NT™ standard treated capillaries, scanned at fixed
505 temperature of 37°C where the excitation power was fixed at 60%. Dose - response curves obtained by plotting the fraction
506 bound of merged data of experimental sets of 16 capillaries (n=3) as function of ligand concentration using MO analysis
507 software (v2.3). Error bars represent standard deviation of the average of three values for each concentration.

508
509

510 5 Conclusion

511 The interaction study between large biomolecules (protein) and small ligands requires extremely sensitive
512 techniques to determine the minuscule variation occurring during the binding. MST, a novel biophysical
513 technique, has demonstrated its capacity to overcome all limitations encountered with conventionnel techniques
514 and specifically the detection limit.

515 In the present work, a systematic study was carried out using MST for the first time to determine the dissociation
516 constant (K_d) between hyaluronidase, a model enzyme, and two small flavonoid compounds known as Hyal's
517 inhibitors. Buffer composition, an important key in different steps of MST experiments, was thoroughly
518 optimized. The phosphate ammonia buffer at pH 6.6 demonstrated its efficiency for hyaluronidase labelling in
519 terms of nature (amine free) and pH even if an alkaline pH (optimum pH for dye chemistry around 8.2) was

520 avoided to prevent the irreversible Hyal precipitation (pI of hyaluronidase \approx 8.6). The same buffer was used for
521 MST experiments where 0.05% of surfactant, Tween-20, was added to efficiently prevent enzyme adsorption
522 and aggregations when using uncoated capillaries. Considering its complicated working and inhibition
523 mechanism, the preservation of hyaluronidase's catalytic activity after labelling was crucial to check. Using only
524 few tens of nM, Hyal* activity was verified and confirmed by pre-capillary CE assay. CE results have proven the
525 sensitivity of CE and the importance of using it among other techniques complementary to MST.
526 To carry out MST experiments, Hyal* concentration was selected according to fluorescence signal intensity and
527 shape. 5 nM was found to be largely sufficient, demonstrating the excellent sensitivity of the technique.
528 Moreover, to correlate the changing of thermophoretic signal to the labelled enzyme state (bound or unbound)
529 exclusively, the absence of ligand intrinsic fluorescence is mandatory which was confirmed in our case. Finally,
530 the dissociation constants (K_d) between small compounds and Hyal* were determined in the presence of Hyal*'s
531 substrate, HA at 0.4 μ M. The values were equal to 163 μ M for Hyal*/HA/EGCG and 157 μ M for
532 Hyal*/HA/apigenin-7-glucoside. The binding affinity results have demonstrated the complexity of the inhibition
533 mechanism of these small molecules towards hyaluronidase where an allosteric inhibition mode was identified.
534 MST as well as CE are sensitive and provided complementary information allowing thereafter a better
535 understanding of biomolecular binding affinity. In the very near future, we intend to explore further the
536 inhibition mechanism and to use MST for screening various natural and synthetic compounds towards
537 hyaluronidase.

538 **Funding information**

539 This work has been financially supported by Université d'Orléans, the Région centre Val de Loire and the Labex
540 SynOrg (ANR-11- LABX-0029).

541

542 **Acknowledgements**

543 The authors would like to thank Nanotemper society and more precisely Dr. Pierre Soule and Dr. Mathilde
544 Belnou for technical support.

545

546 **Conflict of interests**

547 The authors declare that they have no conflict of interests.

548

549 **Author contribution**

550 R. Nasreddine planned and performed MST and CE-based enzymatic experiments and analyzed the
551 corresponding data and R. Nehmé managed the project and data analysis. Both authors discussed the results and
552 contributed to the final manuscript.

553

554

556 **6 References**

- 557 [1] R. Perozzo, G. Folkers, L. Scapozza, Thermodynamics of protein-ligand interactions: history, presence,
558 and future aspects, *J. Recept. Signal Transduct. Res.* 24 (2004) 1–52. [https://doi.org/10.1081/rrs-
559 120037896](https://doi.org/10.1081/rrs-120037896).
- 560 [2] H. Su, Y. Xu, Application of ITC-Based Characterization of Thermodynamic and Kinetic Association of
561 Ligands With Proteins in Drug Design, *Front Pharmacol.* 9 (2018) 1133.
562 <https://doi.org/10.3389/fphar.2018.01133>.
- 563 [3] J.M.D. Trani, S.D. Cesco, R. O'Leary, J. Plescia, C.J. do Nascimento, N. Moitessier, A.K. Mittermaier,
564 Rapid measurement of inhibitor binding kinetics by isothermal titration calorimetry, *Nat Commun.* 9
565 (2018) 1–7. <https://doi.org/10.1038/s41467-018-03263-3>.
- 566 [4] Y. Wang, G. Wang, N. Moitessier, A.K. Mittermaier, Enzyme Kinetics by Isothermal Titration
567 Calorimetry: Allostery, Inhibition, and Dynamics, *Front Mol Biosci.* 7 (2020) 583826.
568 <https://doi.org/10.3389/fmolb.2020.583826>.
- 569 [5] K.S. Phillips, Q. Cheng, Recent advances in surface plasmon resonance based techniques for bioanalysis,
570 *Anal Bioanal Chem.* 387 (2007) 1831–1840. <https://doi.org/10.1007/s00216-006-1052-7>.
- 571 [6] X. Guo, Surface plasmon resonance based biosensor technique: a review, *J Biophotonics.* 5 (2012) 483–
572 501. <https://doi.org/10.1002/jbio.201200015>.
- 573 [7] C.M. Miyazaki, F.M. Shimizu, J.R. Mejía-Salazar, O.N. Oliveira, M. Ferreira, Surface plasmon resonance
574 biosensor for enzymatic detection of small analytes, *Nanotechnology.* 28 (2017) 145501.
575 <https://doi.org/10.1088/1361-6528/aa6284>.
- 576 [8] J. Xue, Y. Bai, H. Liu, Hybrid methods of surface plasmon resonance coupled to mass spectrometry for
577 biomolecular interaction analysis, *Anal Bioanal Chem.* 411 (2019) 3721–3729.
578 <https://doi.org/10.1007/s00216-019-01906-y>.
- 579 [9] J.L. Ortega-Roldan, M. Blackledge, M.R. Jensen, Characterizing Protein-Protein Interactions Using
580 Solution NMR Spectroscopy, in: J.A. Marsh (Ed.), *Protein Complex Assembly: Methods and Protocols*,
581 Springer, New York, NY, 2018: pp. 73–85. https://doi.org/10.1007/978-1-4939-7759-8_5.
- 582 [10] G. Wang, Z.-T. Zhang, B. Jiang, X. Zhang, C. Li, M. Liu, Recent advances in protein NMR spectroscopy
583 and their implications in protein therapeutics research, *Anal Bioanal Chem.* 406 (2014) 2279–2288.
584 <https://doi.org/10.1007/s00216-013-7518-5>.
- 585 [11] D.A. Gell, A.H. Kwan, J.P. Mackay, NMR Spectroscopy in the Analysis of Protein-Protein Interactions,
586 in: G.A. Webb (Ed.), *Modern Magnetic Resonance*, Springer International Publishing, Cham, 2017: pp. 1–
587 34. https://doi.org/10.1007/978-3-319-28275-6_121-1.
- 588 [12] S. Varghese, P.J. Halling, D. Häussinger, S. Wimperis, Two-dimensional ¹H and ¹H-detected NMR study
589 of a heterogeneous biocatalyst using fast MAS at high magnetic fields, *Solid State Nuclear Magnetic
590 Resonance.* 92 (2018) 7–11. <https://doi.org/10.1016/j.ssnmr.2018.03.003>.
- 591 [13] P. Schuck, Analytical Ultracentrifugation as a Tool for Studying Protein Interactions, *Biophys Rev.* 5
592 (2013) 159–171. <https://doi.org/10.1007/s12551-013-0106-2>.
- 593 [14] T.R. Patel, D.J. Winzor, D.J. Scott, Analytical ultracentrifugation: A versatile tool for the characterisation
594 of macromolecular complexes in solution, *Methods.* 95 (2016) 55–61.
595 <https://doi.org/10.1016/j.jymeth.2015.11.006>.
- 596 [15] W.A. Lea, A. Simeonov, Fluorescence Polarization Assays in Small Molecule Screening, *Expert Opin
597 Drug Discov.* 6 (2011) 17–32. <https://doi.org/10.1517/17460441.2011.537322>.
- 598 [16] A.M. Rossi, C.W. Taylor, Analysis of protein-ligand interactions by fluorescence polarization, *Nat Protoc.*
599 6 (2011) 365–387. <https://doi.org/10.1038/nprot.2011.305>.
- 600 [17] J. Chen, J. Liu, X. Chen, H. Qiu, Recent progress in nanomaterial-enhanced fluorescence
601 polarization/anisotropy sensors, *Chinese Chemical Letters.* 30 (2019) 1575–1580.
602 <https://doi.org/10.1016/j.cclet.2019.06.005>.
- 603 [18] D.S. Hage, J.A. Anguizola, C. Bi, R. Li, R. Matsuda, E. Papastavros, E. Pfaunmiller, J. Vargas, X. Zheng,
604 Pharmaceutical and biomedical applications of affinity chromatography: recent trends and developments, *J
605 Pharm Biomed Anal.* 69 (2012) 93–105. <https://doi.org/10.1016/j.jpba.2012.01.004>.
- 606 [19] S. Iftekhhar, S.T. Ovbude, D.S. Hage, Kinetic Analysis by Affinity Chromatography, *Front Chem.* 7
607 (2019). <https://doi.org/10.3389/fchem.2019.00673>.
- 608 [20] C. Zhang, E. Rodriguez, C. Bi, X. Zheng, D. Suresh, K. Suh, Z. Li, F. Elsebaei, D.S. Hage, High
609 Performance Affinity Chromatography and Related Separation Methods for the Analysis of Biological and
610 Pharmaceutical Agents, *Analyst.* 143 (2018) 374–391. <https://doi.org/10.1039/c7an01469d>.
- 611 [21] X. He, Y. Ding, D. Li, B. Lin, Recent advances in the study of biomolecular interactions by capillary
612 electrophoresis, *Electrophoresis.* 25 (2004) 697–711. <https://doi.org/10.1002/elps.200305727>.

- 613 [22] R. Nehmé, C. Perrin, H. Cottet, M.D. Blanchin, H. Fabre, Influence of polyelectrolyte coating conditions
614 on capillary coating stability and separation efficiency in capillary electrophoresis, *Electrophoresis*. 29
615 (2008) 3013–3023. <https://doi.org/10.1002/elps.200700886>.
- 616 [23] H. Nehmé, R. Nehmé, P. Lafite, S. Routier, P. Morin, New development in in-capillary electrophoresis
617 techniques for kinetic and inhibition study of enzymes, *Anal. Chim. Acta*. 722 (2012) 127–135.
618 <https://doi.org/10.1016/j.aca.2012.02.003>.
- 619 [24] D. El-Hady, S. Kühne, N. El-Maali, H. Wätzig, Precision in affinity capillary electrophoresis for drug–
620 protein binding studies, *Journal of Pharmaceutical and Biomedical Analysis*. 52 (2010) 232–241.
621 <https://doi.org/10.1016/j.jpba.2009.12.022>.
- 622 [25] A.C. Moser, S. Trenhaile, K. Frankenberg, Studies of antibody-antigen interactions by capillary
623 electrophoresis: A review, *Methods*. 146 (2018) 66–75. <https://doi.org/10.1016/j.ymeth.2018.03.006>.
- 624 [26] F. Yu, Q. Zhao, D. Zhang, Z. Yuan, H. Wang, Affinity Interactions by Capillary Electrophoresis: Binding,
625 Separation, and Detection, *Anal Chem*. 91 (2019) 372–387.
626 <https://doi.org/10.1021/acs.analchem.8b04741>.
- 627 [27] C. Zhang, A.G. Woolfork, K. Suh, S. Ovbude, C. Bi, M. Elzoeiry, D.S. Hage, Clinical and pharmaceutical
628 applications of affinity ligands in capillary electrophoresis: A review, *Journal of Pharmaceutical and
629 Biomedical Analysis*. 177 (2020) 112882. <https://doi.org/10.1016/j.jpba.2019.112882>.
- 630 [28] C.J. Wienken, P. Baaske, U. Rothbauer, D. Braun, S. Duhr, Protein-binding assays in biological liquids
631 using microscale thermophoresis, *Nat Commun*. 1 (2010) 1–7. <https://doi.org/10.1038/ncomms1093>.
- 632 [29] L. Khavrutskii, J. Yeh, O. Timofeeva, S.G. Tarasov, S. Pritt, K. Stefanisko, N. Tarasova, Protein
633 Purification-free Method of Binding Affinity Determination by Microscale Thermophoresis, *J Vis Exp*.
634 (2013). <https://doi.org/10.3791/50541>.
- 635 [30] C. Entzian, T. Schubert, Studying small molecule–aptamer interactions using MicroScale Thermophoresis
636 (MST), *Methods*. 97 (2016) 27–34. <https://doi.org/10.1016/j.ymeth.2015.08.023>.
- 637 [31] T. Bartoschik, S. Galinec, C. Kleusch, K. Walkiewicz, D. Breitsprecher, S. Weigert, Y.A. Muller, C. You,
638 J. Piehler, T. Vercruyse, D. Daelemans, N. Tschammer, Near-native, site-specific and purification-free
639 protein labeling for quantitative protein interaction analysis by MicroScale Thermophoresis, *Sci Rep*. 8
640 (2018) 1–10. <https://doi.org/10.1038/s41598-018-23154-3>.
- 641 [32] T. Mrozowich, V. MeierStephenson, T.R. Patel, Microscale thermophoresis: warming up to a new
642 biomolecular interaction technique, *Biochem (Lond)*. 41 (2019) 8–12.
643 <https://doi.org/10.1042/BIO04102008>.
- 644 [33] N. Lee, S. Wiegand, Thermophoretic Micron-Scale Devices: Practical Approach and Review, *Entropy*. 22
645 (2020) 950. <https://doi.org/10.3390/e22090950>.
- 646 [34] M. Asmari, R. Ratih, H.A. Alhazmi, S. El Deeb, Thermophoresis for characterizing biomolecular
647 interaction, *Methods*. 146 (2018) 107–119. <https://doi.org/10.1016/j.ymeth.2018.02.003>.
- 648 [35] M. Jerabek-Willemsen, C.J. Wienken, D. Braun, P. Baaske, S. Duhr, Molecular Interaction Studies Using
649 Microscale Thermophoresis, *ASSAY and Drug Development Technologies*. 9 (2011) 342–353.
650 <https://doi.org/10.1089/adt.2011.0380>.
- 651 [36] T.C. Laurent, J.R. Fraser, Hyaluronan, *FASEB J*. 6 (1992) 2397–2404.
- 652 [37] J.R. Fraser, T.C. Laurent, U.B. Laurent, Hyaluronan: its nature, distribution, functions and turnover, *J.
653 Intern. Med*. 242 (1997) 27–33. <https://doi.org/10.1046/j.1365-2796.1997.00170.x>.
- 654 [38] J.M. Cyphert, C.S. Trempus, S. Garantziotis, Size Matters: Molecular Weight Specificity of Hyaluronan
655 Effects in Cell Biology, *Int J Cell Biol*. 2015 (2015). <https://doi.org/10.1155/2015/563818>.
- 656 [39] K. Masuko, M. Murata, K. Yudoh, T. Kato, H. Nakamura, Anti-inflammatory effects of hyaluronan in
657 arthritis therapy: Not just for viscosity, *Int J Gen Med*. 2 (2009) 77–81.
658 <https://www.ncbi.nlm.nih.gov/pmc/articles/PMC2840553/> (accessed April 13, 2020).
- 659 [40] A. Fakhari, C. Berkland, Applications and Emerging Trends of Hyaluronic Acid in Tissue Engineering, as
660 a Dermal Filler, and in Osteoarthritis Treatment, *Acta Biomater*. 9 (2013) 7081–7092.
661 <https://doi.org/10.1016/j.actbio.2013.03.005>.
- 662 [41] M. Corbett, D. Marshall, M. Harden, S. Oddie, R. Phillips, W. McGuire, Treatment of extravasation
663 injuries in infants and young children: a scoping review and survey, *Health Technol Assess*. 22 (2018) 1–
664 112. <https://doi.org/10.3310/hta22460>.
- 665 [42] E.V. Maytin, Hyaluronan: More than just a wrinkle filler, *Glycobiology*. 26 (2016) 553–559.
666 <https://doi.org/10.1093/glycob/cww033>.
- 667 [43] S. Helm Ii, G. Racz, Hyaluronidase in Neuroplasty: A Review, *Pain Physician*. 22 (2019) 555–560.
- 668 [44] G.C. Weber, B.A. Buhren, H. Schrupf, J. Wohlrab, P.A. Gerber, Clinical Applications of Hyaluronidase,
669 *Adv Exp Med Biol*. 1148 (2019) 255–277. https://doi.org/10.1007/978-981-13-7709-9_12.
- 670 [45] R. Nasreddine, L. Orlic, G. Al Hamoui Dit Banni, S. Fayad, A. Marchal, F. Piazza, C. Lopin-Bon, J.
671 Hamacek, R. Nehmé, Polyethylene glycol crowding effect on hyaluronidase activity monitored by

- 672 capillary electrophoresis, *Anal Bioanal Chem.* 412 (2020) 4195–4207. [https://doi.org/10.1007/s00216-](https://doi.org/10.1007/s00216-020-02659-9)
673 020-02659-9.
- 674 [46] S. Fayad, R. Nehmé, M. Langmajerová, B. Ayela, C. Colas, B. Maunit, J.-C. Jacquinet, A. Vibert, C.
675 Lopin-Bon, G. Zdeněk, P. Morin, Hyaluronidase reaction kinetics evaluated by capillary electrophoresis
676 with UV and high-resolution mass spectrometry (HRMS) detection, *Anal Chim Acta.* 951 (2017) 140–
677 150. <https://doi.org/10.1016/j.aca.2016.11.036>.
- 678 [47] S. Fayad, B. Ayela, C. Chat, P. Morin, C. Lopin-Bon, R. Nehmé, Effect of modified di- and trisaccharides
679 on hyaluronidase activity assessed by capillary electrophoresis-based enzymatic assay, *Carbohydr Res.*
680 475 (2019) 56–64. <https://doi.org/10.1016/j.carres.2019.02.006>.
- 681 [48] R. Nehmé, R. Nasreddine, L. Orlic, C. Lopin-Bon, J. Hamacek, F. Piazza, Kinetic theory of hyaluronan
682 cleavage by bovine testicular hyaluronidase in standard and crowded environments, *Biochimica et*
683 *Biophysica Acta (BBA) - General Subjects.* 1865 (2021) 129837.
684 <https://doi.org/10.1016/j.bbagen.2020.129837>.
- 685 [49] Kd Fit Model - Definition and Relevance | Nanopedia, NanoTemper Technologies.
686 <https://nanotempertech.com/nanopedia/kd-fit-model/> (accessed August 12, 2021).
- 687 [50] L. Hellinen, S. Bahrpeyma, A.-K. Rimpelä, M. Hagström, M. Reinisalo, A. Urtili, Microscale
688 Thermophoresis as a Screening Tool to Predict Melanin Binding of Drugs, *Pharmaceutics.* 12 (2020) 554.
689 <https://doi.org/10.3390/pharmaceutics12060554>.
- 690 [51] H.E. Alburn, R.W. Whitley, Factors affecting the assay of hyaluronidase, *Journal of Biological Chemistry.*
691 192 (1951) 379–393. [https://doi.org/10.1016/S0021-9258\(18\)55942-1](https://doi.org/10.1016/S0021-9258(18)55942-1).
- 692 [52] H. Bisswanger, *Enzyme Kinetics: Principles and Methods*, John Wiley & Sons, 2017.
- 693 [53] S. Patil, B. Bhadane, L. Shirsath, R. Patil, B. Chaudhari, Steroidal fraction of *Carissa carandas* L. inhibits
694 microbial hyaluronidase activity by mixed inhibition mechanism, *Preparative Biochemistry &*
695 *Biotechnology.* 49 (2019) 298–306. <https://doi.org/10.1080/10826068.2018.1541811>.
- 696 [54] K. Tomohara, T. Ito, S. Onikata, A. Kato, I. Adachi, Discovery of hyaluronidase inhibitors from natural
697 products and their mechanistic characterization under DMSO-perturbed assay conditions, *Bioorg Med*
698 *Chem Lett.* 27 (2017) 1620–1623. <https://doi.org/10.1016/j.bmcl.2017.01.083>.